High Strain Rate and Impact Experiments

Afonso José de Vilhena Leitão Gregório
afonsogregorio@tecnico.ulisboa.pt
Instituto Superior Técnico, Universidade de Lisboa, Portugal
November 2017

Abstract

This document presents a comprehensive investigation on plastic flow of metals at high strain rates. The experimental development consisted of projecting and manufacturing testing machines, but alto of integrating transducers developed for high-speed applications. The test plan comprised a group of pure and commercially pure metals (Aluminium, Copper, Zinc, Tin, AA1085 and AA1050) and a group of alloys that is representative of industrial applications (AlSi9Cu3, AS7G03, AISI1045 and Ti6Al4V), which were tested to high strains, at high strain rates of up to $1{,}5\times10^{4}\ s^{-1}$. The results present and discuss the parameters that have influence on the mechanical resistance of materials for different strain rate conditions, seeking to contribute for a better understanding of viscoplasticity in metallic materials but also to suggest new techniques and methodologies for high strain rate mechanical testing.

Keywords: Strain rate, flow stress, pure metals, engineering alloys, mechanical characterization.

1 Introduction

Metals are widely used for production of components and goods. Throughout their transformation, materials undergo several mechanical processing phases, which comprise cutting and/or forming processes. Due to the kinematic nature of the tools involved in these processes, materials experience plastic deformation under a wide range of strain rates[1], being the strain rate a major factor on the mechanical behaviour of materials, particularly in their flow stress[2]. Therefore, when modelling an industrial process, strain rate is of major importance and must be taken into account.
There is, however, a lack of information on the mechanical behaviour of materials for high strains at high strain rates. If there is a considerable amount of information for quasi-static conditions, the same is not true for the above-mentioned case as such conditions are usually not available in literature or databases[3]. This is particularly relevant since all analytical and numerical modelling techniques are dependent on this information to calibrate empirical models[4]. Therefore, the lack of information on material characterization conducted under the real conditions that materials experience is the main source of errors when modelling technological processes.

There are several machines and techniques that allow conducting experiments under different strain rates. For: *(i)* very low strain rates of up to $1\ s^{-1}$ there are universal testing machines; for *(ii)* intermediate strain rates ($1-10^{2}\ s^{-1}$) there are drop hammers and hydraulic/mechanic based systems[5], [6], [7] ; and for *(iii)* high strain rates (over $10^{2}s^{-1}$) there are Split Hopkinson Pressure Bars and Taylor impact devices[8].
However, only a scarce number of the above-mentioned machines can replicate the stress rate-strain conditions of real processes. Furthermore, the ones that can are often associated with results' uncertainty, hence the need for development and better understanding on material characterization at high strain rates.

2 Materials and Procedures

2.1 Materials

For the present work were selected materials from two different groups: *(i)* pure and commercially pure metals and *(ii)* engineering alloys representative of industrial applications. The first group comprises Aluminium,

Copper, Zinc, Tin, AA1085 and AA105, which were used to validate the machines and procedures developed by the author. The use of metals in its purest form makes it easier to compare the results of tests conducted by different laboratories against the results presented in literature since these are less susceptible to metallurgic variations. High purity metals also present higher ductility and are softer when compared to alloys, resulting in less mechanical demand on the prototype machines developed during this work.

The selected group of engineering alloys comprises materials representative of the following industrial applications: *(i)* extrusion, casting and injected casting; *(ii)* forging, bending and welded construction; and *(iii)* machining of components serving biomedical and aeronautic purposes. In representation of the first mentioned application, following APF (Associação Portuguesa de Fundição) guidelines, were chosen *(i)* AlSi9Cu3 and *(ii)* AS7G03+05U. Regarding the second application, was chosen, according to CMM (Associação Portuguesa de Construção Metálica e Mista) guidelines, the medium carbon steel AISI1045. Whereas the titanium super alloy Ti6Al4V was chosen according to the study group "Cooperative Work on Material Constitutive Models and Data for Modelling of Metal Cutting" from CIRP STC-C (The International Academy for Production Engineering – Cutting) in representation of the third mentioned application.

Of all the selected materials, special emphasis was given to Aluminium and its alloys since it is one of the most well documented metals in the literature, and also to the titanium super alloy Ti6Al4V due to its high strength and hardness.

Cylindrical specimens of 6 *mm* in diameter and 6,4 *mm* in height were produced from all the presented materials. Specimens of pure and commercially pure metals were then annealed, apart from tin, which recrystallizes at room temperature[9].
Due to unknown metallurgic condition of the supplied alloys AISI1045 and Ti6Al4V, special care was taken when preparing specimens of these materials. Discs of 7 *mm* in height were cut out of the supplied 80 *mm* diameter round blocks. Specimens were obtained from the discs using wire-cut EDM process. Plain and cylindrical grinding and fine machining operations were then performed to ensure proper geometry and dimensions. Since no information was provided on the homogeneity of the supplied blocks of AISI1045 and Ti6Al4V, the radial coordinate of all specimens was registered in the form of a matrix to vouch the quality of the present investigation.

Figure 1 – Specimens for uniaxial compression with initial diameter $\emptyset_0 = 6\ mm$ and initial height $h_0 = 6{,}4\ mm$. From left to right: (i) pure Aluminium, (ii) pure Copper, (iii) pure Zinc, (iv) pure Tin, (v) AA1085, (vi) AA1050, (vii) AS7G03+05U, (viii) AISI1045 and (ix) Ti6Al4V.

Once produced all specimens, their top and bottom faces were polished to a shiny surface so that it was possible to accurately measure their Vickers hardness prior to mechanical testing. Vickers hardness tests were carried out using a Hardruler HVS-1000 micro-indentation machine. These tests were used as a quality control test to assess if the specimens of pure and commercially pure metals were in the annealed condition.

2.2 Mechanical Characterization

To investigate the mechanical behaviour of the selected materials under different strain rates, two types of tests were conducted, *(i)* compression tests and *(ii)* Vickers micro-hardness tests. These tests were carried for a vast range of strain rates, from the quasi-static condition to strain rates of up to $1{,}5\times10^4\ s^{-1}$.

From the compression tests, true strain was calculated as:

$$\varepsilon = -\int_{h_0}^{h} \frac{dh}{h} = ln\frac{h_0}{h} \tag{1}$$

And true stress was calculated as:

$$\sigma_r = \frac{F}{A_i} \tag{2}$$

Where A_i, the instant area of the specimen, is given by:

$$A_i = \frac{V}{h_i} = \frac{A_0 h_0}{h_i} = \frac{\pi\left(\frac{\emptyset_0}{2}\right)^2 h_0}{h_0 - d_i} \tag{3}$$

These results were then plotted to obtain the monotonic and incremental flow stress curves for each of the presented materials.
Micro-hardness tests were carried between increments for all incremental compression tests performed on quasi-static conditions. For monotonic compression tests carried throughout the entire range of covered strain rates, only the initial and final hardness values were measured.

2.3 Data Acquisition

Data acquisition (DAQ) and conditioning systems, require special attention when the events intended to analyse occur during a very short time period[10]. Signal conditioning must be fast and sensitive enough to any response in the transducers used to measure the physical parameters of a process, particularly when there is the need of amplifying a weak signal or when the signal must be restricted to a certain maximum value.

Data acquisition is usually carried digitally. Therefore, an analogic to digital converter needs to be present in the acquisition system. For high-speed applications, it is imperative that the converter has a fast response – since the electronic components are often the ones responsible for limitations in what comes to high acquisition rates. The converter is also responsible for the precision and resolution of the DAQ system.

In the present investigation was used a PCI 6115 DAQ board, manufactured by National Instruments (NI). This board allows the simultaneous acquisition of four channels of up to 10MHz, 16MS, 12 bits and 42V. It was then connected to a connection box, model BNC-2120, also from the manufacturer NI. The board control was carried out using specific software – in the case, Labview, which also allows exportation of the signals to an ASC type file.

The DAQ board configuration considered: *(i)* the acquisition rate, seeking for a minimum of 150 experimental points and no more than 300 per test; *(ii)* the adjustment of the measure range, for highest resolution; *(iii)* the signal type – DC; *(iv)* the differential electrical circuit of the analogical to digital converter; and *(v)* the use of filters – in the present case no filters were used, so that the registered values were as accurate as possible.
The data acquisition apparatus comprised all the equipment required to condition, monitor and acquire the physical parameters, force and displacement, of the compression tests.

3 Experimental Development

3.1 Compression Tool

In order to perform uniaxial compression tests, a compression tool was projected and developed. During the project, it was taken into account the difficulties that come when comparing results from different testing machines. Thus, the present tool was projected so it could operate in different testing machines, without further care neither on tribological conditions (related to the compression platens) nor on the instrumentation.

The tool was first modelled using CAD (Computer Aided Design) software, as presented in Figure 2.

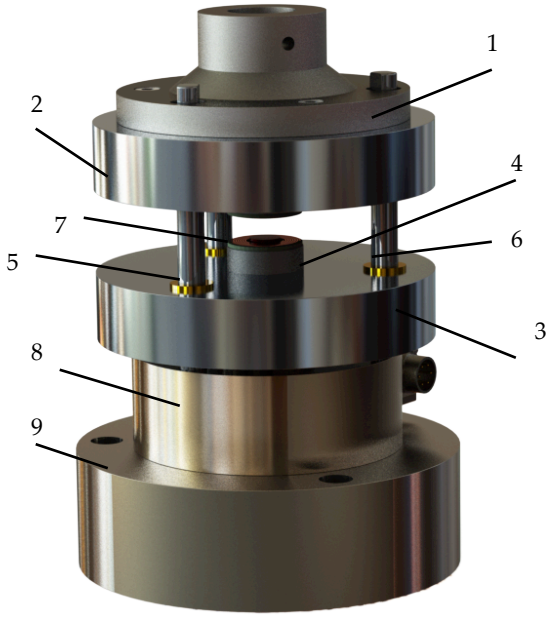

Figure 2 – Compression tool, modelled in Solidworks. ***1*** *– Connector;* ***2*** *– Top Platen Holder;* ***3*** *– Bottom Platen Holder;* ***4*** *– Compression Platen;* ***5*** *- Bushing;* ***6*** *– Guide Column;* ***7*** *– Displacement Sensor;* ***8*** *– Load Cell;* ***9*** *– Tool base.*

As seen above, the tool features two groups of components: *(i)* the mechanical components, which control the movement and alignment between compression platens; and *(ii)* electrical components, which are responsible for measuring the physical parameters (time,

force and displacement) involved in the testing processes. Of extreme importance is the set bushings (5) – guiding columns (6), since it is responsible for a smooth movement between the two plates (2 and 3) that hold the compression platens (4), and consequently, for proper transmission of force to the specimen and load cell.

The compression platens are the component that must withstand, without deforming, all the forces involved in the compression tests.
The first set of platens was made of forged steel and proved to be inadequate for the compression of AISI1045 and Ti6Al4V, reason why a second pair of platens were designed, made of tungsten carbide. Since WC is a hard metal, it is very difficult, via conventional methods, to cut or polish. Thus, after assembly, the platens' surface planicity was achieved with resource to a plain grinder. This set of platens was then meticulously polished to a mirror like finish (Figure 3 (a)) using a diamond compound. The polishing procedure is important because, otherwise, the directional scratches left by the grinding process won't allow the specimens' deformation to be axisymmetric, resulting in high stress concentration zones that can lead to crack propagation (Figure 3 (c)). The hard metal platens performed well until subjected to impact, case in which they would break, due to WC´s low fracture toughness (Figure 3 (b)).

(a) (b) (c)

Figure 3 – (a) Tungsten carbide platen; (b) Broken tungsten carbide platen, post impact; (c) Cracked surface under microscope.

For this reason, a final set of platens was made from HSS M2 (Molybdenum High Speed Steel), featuring high tensile strength at higher fracture toughness, making them suitable for all materials even when subjected to impacts.
When projecting the compression tool, it was also taken into account positioning aspects related to *(i)* the force transducers and, *(ii)* the displacement transducers.

A SENSOTEC model 43 load cell was used to measure force. It is based on the principle of resistive transducers of the type full Wheatstone bridge. The load cell was then connected to a VISHAY 2310B amplifier and a gain of 500 was used on the output signal of the cell, which was calibrated via direct application of weights with calibrated mass. The calibration curve was $3mv/V$ when an excitation of 10 V DC was provided. The output signal was then received by the data acquisition board.

The distance between compression platens was measured using a high precision displacement sensor specially designed for high-speed applications. It works on the technology of inductive transducers, based on electromagnetic induction between coils. These coils were assembled in the tool, as close to the compression area as possible, to minimize electromagnetic coupling between the load cell and coil´s signal, but also to assure the accuracy of the measurements since the elastic deformation of the entire tool system doesn't affect the measurement zone of the displacement transducer.
The emitting coil was connected to a function generator TG120, from the manufacturer Thurbly Thandar Instruments, and excited with a square signal at 990 KHz and 10 V_{pk-pk}.

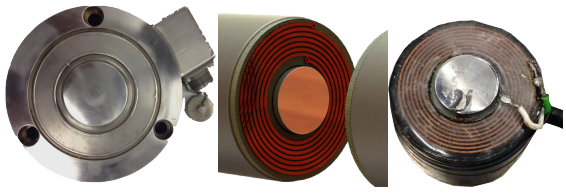

(a) (b) (c)

Figure 4 – (a) Load Cell; (b) Electromagnetic induction principle applied to displacement sensors(c) Implemented displacement sensor.

The signal induced on the receiving coil was, therefore, AC. However, AC signals are not easy to work with, and data acquisition equipment is usually prepared to run on DC signals. Thus, an AC-DC rectifier was developed, which was comprised of 4 diodes assembled in a bridge rectifier. Even though the bridge was beneficial, the signal was still fluctuating around an intermediate voltage value - function of the relative position of the sensors. Capacitive elements were then added to the circuit. It was observed that these

provided the so needed DC signal but had a direct influence on the increase in response time of the sensors, making them of no use for high-speed applications. As a result, it was necessary to establish a trade-off between the quality of the signal and the speed of the rectifier's response. Hence, two rectifiers were developed: *(i)* one to operate in quasi-static conditions and (*ii)* another one for compression tests carried at medium and high speed conditions. A faster response rectifier was achieved by reducing its capacitance and adding a dissipative component, a resistance. Electrical circuits for both rectifiers are presented in figure 5.

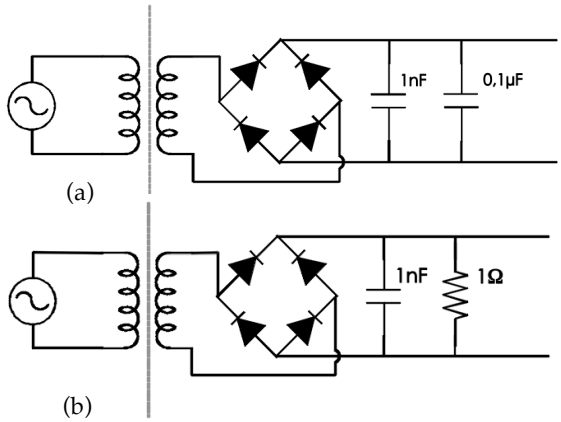

Figure 5 –Electrical circuits for: (a) Quasi-static compression tests (b) Medium and high speed compression tests.

The calibration of induction type sensors features two stages: *(i)* optimization of the excitation parameters, and *(ii)* making a calibration curve that correlates the physical distance to the sensors' electrical response.

Due to the diodes inverse response time, magnetic coupling between force and displacement transducers, and quality of the induced signal in the receiving coil, the excitation parameters were set, as already mentioned, as a square wave at 990 KHz and 10 V_{pk-pk}.

The calibration curve was obtained via incremental compressions of an aluminium specimen. Its height was measured, as well as the corresponding electrical response in Volts for each increment. The calibration curve for this type of transducers is highly non-linear, hence, the calibration range must be between the maximum and minimum height of the specimens during compression tests to avoid extrapolation of results.

In Figure 6 is shown the calibration curve for the displacement sensor.

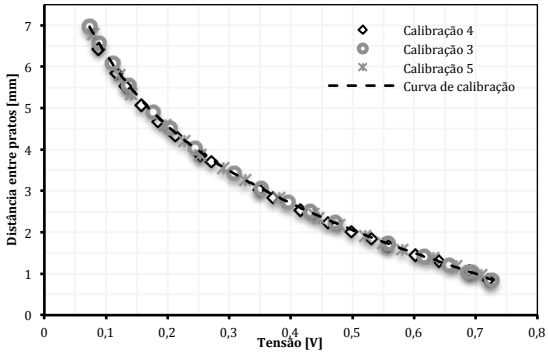

Figure 6 – Calibration curve for the displacement sensor for distances between 1 and 7mm.

3.2 Testing Machines

Contrary to what is desired, there is no testing machine able to conduct compression tests for such a wide range of strain rates. Therefore, it is the present work's objective to develop three different testing machines for different velocity conditions. Thus, were developed/installed: *(i)* a hydraulic press for quasi-static compression tests (velocities of up to 0,1 m/s); (*ii)* a drop hammer for medium velocities (between 1 and 8 m/s); and, *(iii)* a pneumatic cannon for high velocities (over 8 m/s).

Hydraulic Press

A 30T press, by CIATA, was modified and installed in LabM3 (Laboratório de Maquinagem e Micro-fabrico) at IST. Its maximum force and speed are, respectively, 30 ton-force and 0,01 m/s. This machine-tool was adapted to receive the compression tool, and a pressure transducer was also installed in the hydraulic tubing. The hydraulic group of the press was then detached from the main metallic structure to minimize possible interferences external to the compression tests. The schematic of the apparatus is shown in Figure 8 (a).

Drop Hammer

A drop hammer, based on the principle of a falling mass, was installed in LabM3. It is composed by three welded tubes of 200, 100 and 50 mm quadrangular cross sections that promote the guided fall of weights from a maximum height of 3 m. This machine-tool was projected to operate with weights in the range of 1 to 100 Kg, which were heaved using

an electrical-powered winch. The available energy E_p is determined by the mass M of the weight and its height H, whereas the impact velocity is only function of the height, per equations 4 and 5, respectively.

$$E_p = MgH \quad (4)$$

$$v = \sqrt{2gH} \quad (5)$$

So, the maximum impact speed of the developed drop hammer is approximately 8 m/s. The impact energy is of major importance to prevent failure of the tool components, reason why a table with reference operating values is provided.

Table 1 – Reference values for the developed drop hammer.

	Tube		
	1	**2**	**3**
Cross-section [mm]	200x200	100x100	50x50
Lifting weight [Kg]	33 / 66 / 99	10	1
Min. v **[m/s]**	1	1	1
Max. v **[m/s]**	7,7	7,7	7,7
Max. E_p **[J]**	2912,6	294,2	29,4
Max. H **[m]**	3	3	3
Working Principle	Gravity		

The weights are heaved independently using electromagnets, and are activated only one at a time for safety reasons. To control the height of the weights, a scale in cm was marked on each tube. To operate the machine, a control panel was developed. It allows turning the machine on or off, switching between electromagnets, and actuating the drop system.
The compression tool was then placed underneath the drop hammer, fixed on a steel base with multiple holes for easy positioning among tubes. To absorb the impact of the falling weight, a piece of ertacetal was machined and integrated on the top of the tool. This apparatus is shown in Figure 8 (c).

Pneumatic Cannon

A pneumatic cannon was installed in LabM3 to conduct compression tests at high speed. This machine is composed by a pressure chamber and, a pipe that serves the purpose of guiding a projectile. When a valve is released, the pressurized air flows into the pipe accelerating the projectile. The available energy for the test, E_c, is function of the mass M and the velocity v of the projectile, and needs to be taken into account prior to conducting experiments once that this machine easily accelerates a projectile to velocities up to 100 m/s.

$$E_c = \frac{1}{2}Mv^2 \quad (6)$$

To do so, a set of projectiles of different mass is required. Following this principle, it was implemented an impact system in which a projectile strikes on an intermediate bar that then compresses the specimen. The weight ratio between projectile and intermediate bar is responsible for controlling the impact velocity and, therefore, energy.

The pneumatic cannon was installed, horizontally, on a beam. The intermediate bar was aligned with the cannon pipe and placed between a lubricated acrylic bushing for guiding and low friction purposes. To use the same compression tool in this apparatus, the top section of the tool was removed and the left-out compression platen was attached to the intermediate bar. The schematic for this apparatus can be seen in Figure 8 (b).

To estimate the impact velocity as a function of the air pressure inside the pressure chamber, a device was developed. This device made use of two photodiodes and two laser beams, in parallel. The distance between photodiodes was 15 mm, and the signal that they received from the lasers was graphically displayed in a Tektronix TDS220 oscilloscope. By knowing the time that took the intermediate bar to cut through both laser beams, an average velocity could be calculated for that course of 15 mm. The calibration curve is presented below.

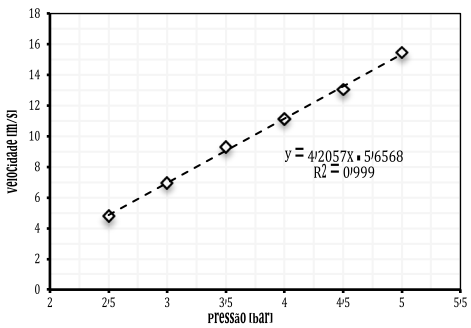

Figure 7 – pressure-velocity calibration curve for the pneumatic cannon, between 2,5 and 5 bar.

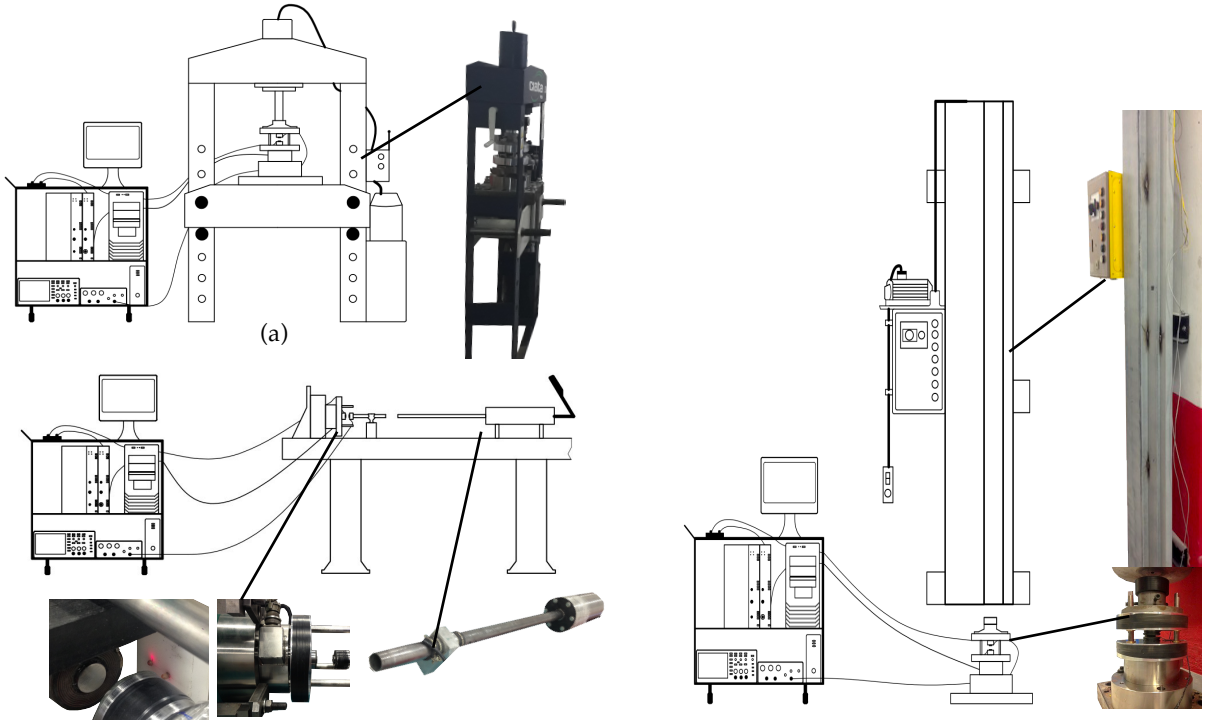

(a) (b) (c)

Figure 8 – Schematic representation and integration of all three apparatus: (a) Hydraulic Press; (b) Pneumatic Cannon; (c) Drop Hammer.

3.3 Test Plan

The test plan consisted in conducting, simultaneously, compression and hardness tests on the selected materials. Hardness tests were performed both as quality control tests and as a way of perceiving differences between the instant flow stress and the yield stress in reloading. Incremental and monotonic compression tests were conducted to evaluate strain rate influence on pure metals and alloyed metals. The parameters used in these mechanical tests allow strains up to 1, at strain rates up to $1{,}5\times10^{4}\ s^{-1}$.

4 Results and Discussion

In order to validate the compression tool developed during this project and accredit its results, compression tests were conducted on a specimen of AA1050 to reproduce the results obtained by Alcino Reis (2016). The specimens had the same dimensions and were collected from the same ingot. Figure 9 shows great concordance and similarity of the results, and served, therefore, as a way of validating both the compression tool and the techniques used to conduct the experiments.

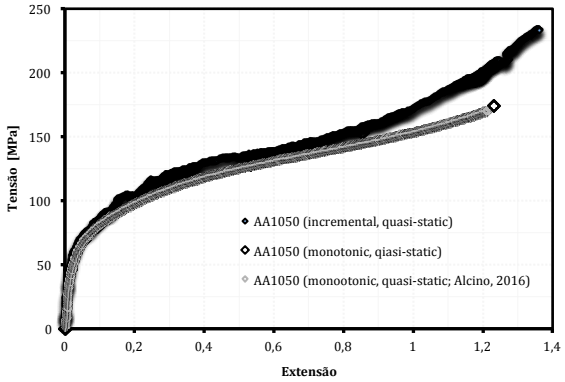

Figure 9 – Comparison between curves for AA1050-O obtain by Alcino Reis and during the present work.

Figure 10 shows hardness – flow stress results for pure metals.

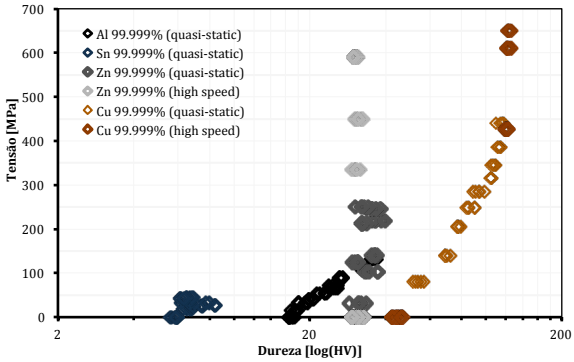

Figure 10 – Hardness vs. flow stress for pure metals after compression.

The flow stress is approximately linear against hardness measurements after compression for quasi-static conditions. However, this relationship doesn´t apply for Zinc as the strain rate increases. At high strain rates, its initial and final hardness is the same. The same happens for Tin. This behaviour occurs due to recrystallization phenomenon promoted by high strain rate deformations as a result of the temperature increase. The observed behaviour is explicit of the need for experimental calibration of the stress-strain relationship for each metal, so that the yield stress can be determined using little intrusive micro hardness tests.

Figure 11 shows initial hardness vs. radial position for Ti6Al4V specimens.

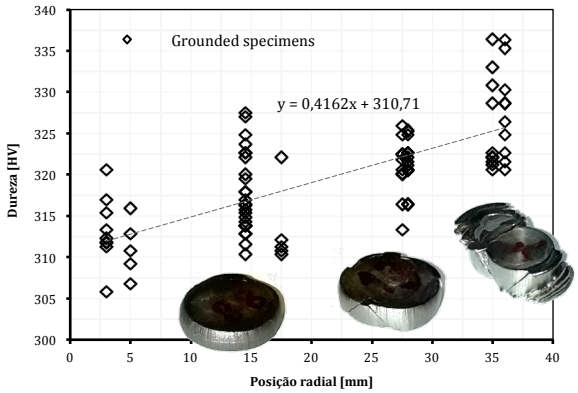

Figure 11 – Initial hardness vs. radial position for Ti6Al4V alloy.

The specimens collected from the centre of the circular block are softer than the ones collected close to the edge. This non-homogeneity is also translated in the deformation mechanism of the tested specimens, as seen on the images overlapped on the graph in figure 11. The specimens from the edge undergo a highly non-homogeneous deformation, whereas the ones from the centre deform in an axisymmetric way. This is representative of why the specimens' preparation is of major importance, and reflects the difficulties to reproduce the same results among different laboratories.

In Figure 12 is shown hardness vs. stress for Aluminium and aluminium alloys, and in Figure 13 is shown hardness vs. stress for all the engineering alloys used in this investigation. 99,999% pure Aluminium is once again used as reference.

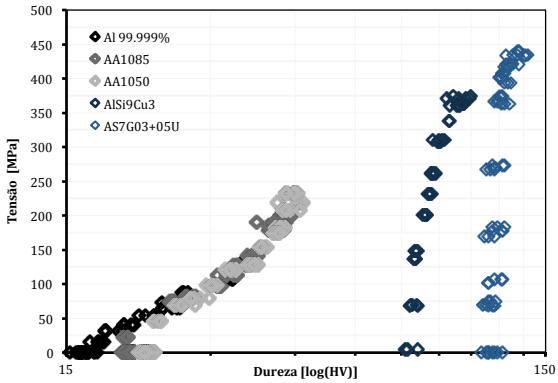

Figure 12 – Hardness vs. stress for Aluminium and its alloys

It's observed that small variations in the alloying elements cause severe differences in the mechanical behaviour of Aluminium. Pure Aluminium (99,999%) has a much lower hardness value than AA1085 (99,85) and AA1050 (99,5), being the respective hardness values 16HV, 20HV, and 22HV. The same happens for the maximum flow stress, with values of 140MPa, 200MPa, and 240MPa, respectively for the above-mentioned materials. However, the hardness-stress relationship doesn't seem to be affected for variations of 0,5% in purity, as opposed to alloys in which the aluminium content is only as high as 93% such as AlSi9Cu3 and AS7G03+05U.

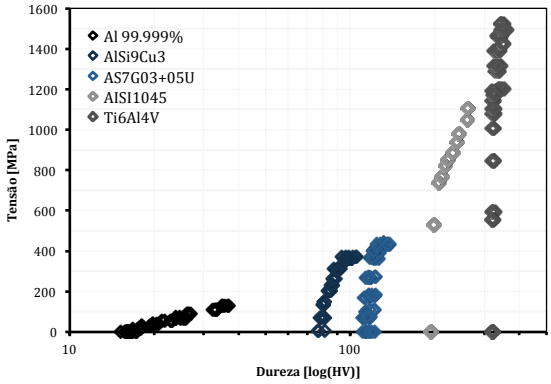

Figure 13 – Hardness vs. stress for engineering alloys

By analysis of Figure 13, it's notorious the steeper slope for hardness-stress curves when the metallurgic condition involves more complex alloying elements (AlSi9Cu3, AS7G03+05Cu and Ti6Al4V) with the purpose of increasing a material's mechanical resistance. This comparison can be made between the two aluminium alloys and pure Aluminium. It's also observed that the less steep slope on the case of pure Aluminium gives a higher resolution for hardness-strain relationship, allowing and encouraging the use

of little intrusive techniques to calculate yield stress and even the amount of deformation that the material has already suffered.

Figure 14 shows flow stress curves for engineering alloys. It´s notorious the increase of mechanical strength of the studied alloys when compared to pure and commercially pure Aluminium, being Ti6Al4V the alloy with the highest flow stress, 10 times superior to the flow stress of AA1050.

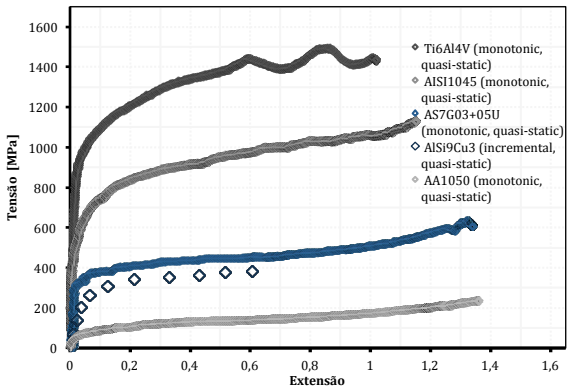

Figure 14 – Flow stress-strain curves for engineering alloys for quasi-static conditions.

Figure 15 presents the flow stress – strain curves for pure Aluminium and AA1050 at different strain rates. Figure 16 presents the same data for pure Zinc.

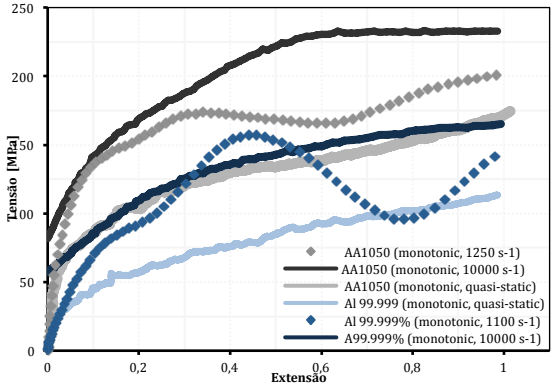

Figure 15 – Flow stress - strain curves for pure Aluminium and AA105, at strain rates of up to 10000^{s-1}.

In figure 15 is shown that, at high strain rates of $10^4\ s^{-1}$, the Aluminium´s flow stress increases 50%. This is of major importance when modelling technological processes, since due to the kinematics of the tools, materials undergo severe strains at high strain rates. If strain rate hardening is not properly considered, never can these processes be modelled in a realistic way, resulting in improper project and manufacture of tools with the purpose of serving the process one is intended to model.

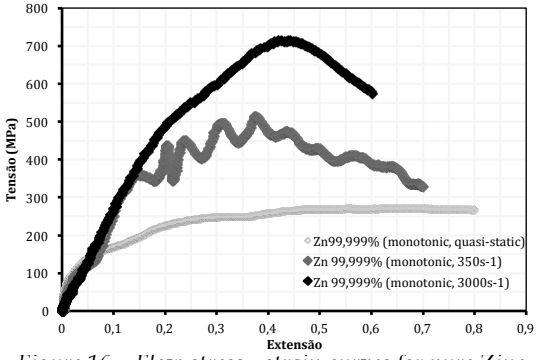

Figure 16 – Flow stress - strain curves for pure Zinc, at strain rates of up to 3000^{s-1}.

Figure 16 shows that different metals exhibit different mechanical behaviour. This is explicit of why there are so many errors when it comes to modelling technological processes. Empirical models that consider always increasing stress must never be used to model the real behaviour of metals such as Zinc, which shows softening for strains above 0,5. It is also observed that Zinc's mechanical resistance at $3\times10^3 s^{-1}$ increases approximately 100% in relation to quasi-static conditions.

In Figures 17 and 18 is shown the flow stress – strain curves for AISI1045 and Ti6Al4V at high strain rates.

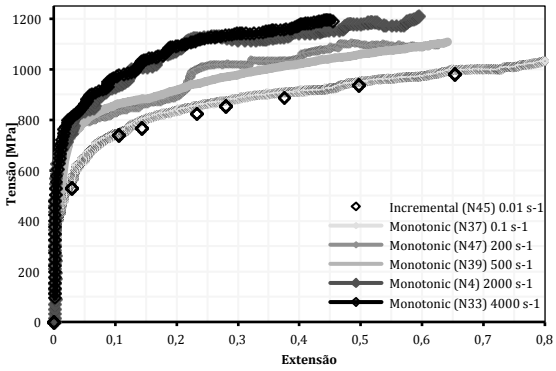

Figure 17 – Flow stress - strain curves for border specimens of AISI1045, at different strain rates.

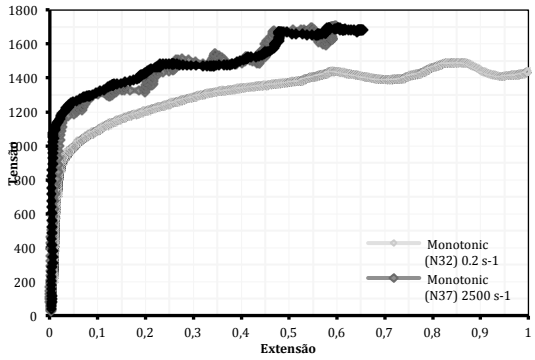

Figure 18 – Flow stress-strain curves for centre specimens of Ti6Al4V, at strain rates of up to 4000^{s-1}.

By analysis of Figures 17 and 18 it's observed that the flow stress of both AISI1045 and Ti6Al4V is influenced by strain rate. The conducted experiments show an increase in flow stress of 50% in AISI1045 and 25% in the case of Ti6Al4V. Even though AISI1045 increases its flow stress by a higher percentage, it is still far below the flow stress of Ti6Al4V for the same strain rate of $4\times10^{3}s^{-1}$. In general terms, Ti6Al4V exhibits higher mechanical resistance than steel (about 40% higher), for a 45% lower density. However, the deformation in the AISI1045 samples is more homogeneous. It's also observed that the flow stress curve for Ti6Al4V has several drastic variations, due to the internal propagation of cracks, since prior to cracking there is an instantaneous relief of force in the compression platens. This cracking mechanism seems to be strain related, since they appear for strains above 0,5.

5 Conclusions

Once finished the present investigation, it's first concluded that the established objectives were fulfilled. Uniaxial compression tests were conducted under a wide range of strain rates, from 10^{-1} to $1{,}5\times10^{4}\ s^{-1}$. To do so, there were successfully developed three testing machines, and also a compression tool that could operate under such demanding conditions, providing results and an insight on the mechanical behaviour of a selected group of materials when subjected to high strain rate compression.

The experimental results show that different materials exhibit different stress – strain responses. Hence the need for empirical models that predict these different responses.

Pure metals and engineering alloys don't increase their mechanical resistance in the same way when subjected to high strain rate deformation.

Hardness tests can be of extreme value to be used as a little intrusive quality control technique. Hardness tests, when coupled with compression tests are also of value for mechanical characterization.

The type of machine used in the experiments at different strain rates has a direct influence on the quality of the flow stress-strain curves. Typical vibrations produced by impact machines introduce noise in the measurements, particularly in the case of the drop hammer.

References

[1] [Guo Y. B. (2003) An integral method to determine the mechanical behaviour of materials in metal cutting, Journal of Materials Processing Technology, 142, 72-81

[2] Clifton RJ. High Strain Rate Behavior of Metals. ASME. *Appl. Mech. Rev.* 1990;43(5S):S9-S22.

[3] Silva C.M.A., Rosa P.A.R. and Martins P.A.F., Innovative Testing Machines and Methodologies for the Mechanical Characterization of Materials, *Experimental Techniques*, 40, 569-581 (2016)

[4] Rosa P.A.R., Cristino V.A.M., Silva C.M.A. e Martins P.A.F., Input Data for the Numerical Simulation of Metal Cutting, *Trans Tech Publications*, *Advanced Materials Research*, **223**, 257-266 (2011)

[5] Diot S., Guines D., Gavrus A., Ragneau E., Two-step procedure for identification of metal behavior from dynamic compression tests, International Journal of Impact Engineering, 34, (2007), 1163-1184

[6] Grässel L.K., Frommeyer G., Meyer L.W., High strength Fe–Mn–(Al, Si) TRIP/TWIP steels development – properties – application, International Journal of Plasticity, 16, (2000), 1391-1409

[7] Wang Z.J., Cheng L.D., Experimental research and numerical simulation of the dynamic cylinder upsetting, Materials Science and Engineering: A, 499, (2009), 138-141.].

[8] Taylor G.I., The use of flat-ended projectiles for determining dynamic yield stress - Theoretical considerations, Proceedings Royal Society London A, 194, (1948), 289-299

[9] Recrystallization Principles Applied to Whisker Growth in TinDr. Irina Boguslavsky, NEMI Consultant Peter Bush, University at Buffalo

[10] Sadeghbeigi, R. (2012). Chapter 2. Process Control Instrumentation Technology. In *Fluid Catalytic Cracking Handbook (Third Edition)* (pp. 43–49). Amsterdam, The Netherlands.: Elsevier Science & Technology Books